

# Center-of-mass energy dependence of intrinsic- $k_T$ distributions obtained from Drell-Yan production

I. Bujanja\*<sup>1,2</sup>, H. Jung<sup>†</sup><sup>3,4</sup>, A. Lelek<sup>‡</sup><sup>5</sup>, N. Raičević<sup>§</sup><sup>1</sup>, and  
S. Taheri Monfared<sup>¶</sup><sup>3</sup>

<sup>1</sup>Faculty of Science and Mathematics, University of Montenegro, Podgorica,  
Montenegro

<sup>2</sup>Interuniversity Institute for High Energies (IIHE), Université libre de Bruxelles,  
Belgium

<sup>3</sup>Deutsches Elektronen-Synchrotron DESY, Germany

<sup>4</sup>II. Institut für Theoretische Physik, Universität Hamburg, Hamburg, Germany

<sup>5</sup>University of Antwerp, Belgium

arXiv:2404.04088v3 [hep-ph] 14 Mar 2025

---

\*itana.bujanja@cern.ch

†hannes.jung@desy.de

‡aleksandra.lelek@uantwerpen.be

§natar@ucg.ac.me

¶sara.taheri.monfared@desy.de

## Abstract

The internal motion of partons inside hadrons has been studied through its impact on very low transverse momentum spectra of Drell-Yan (DY) pairs created in hadron-hadron collisions. We study DY production at next-to-leading order using the Parton Branching (PB) method which describes the evolution of transverse momentum dependent parton distributions. The main focus is on studying the intrinsic transverse momentum distribution (intrinsic- $k_T$ ) as a function of the center-of-mass energy  $\sqrt{s}$ . While collinear parton shower Monte Carlo event generators require intrinsic transverse momentum distributions strongly dependent on  $\sqrt{s}$ , this is not the case for the PB method. We perform a detailed study of the impact of soft parton emissions. We show that by requiring a minimal transverse momentum,  $q_0$ , of a radiated parton, a dependence of the width of the intrinsic- $k_T$  distribution as a function of  $\sqrt{s}$  is observed. This dependence becomes stronger with increasing  $q_0$ .

## 1 Introduction

The transverse momentum distribution of Drell-Yan (DY) lepton pairs,  $p_T(\ell\ell)$ , at large transverse momentum is well described by calculations at higher orders of the strong coupling  $\alpha_s$ , at low transverse momenta of the order of a few GeV the spectrum is described by perturbative resummation, while at very low  $p_T(\ell\ell)$  non-perturbative contributions become important. The resummation region can be treated in form of Transverse Momentum Dependent (TMD) parton distributions or by parton-showers in event generators like HERWIG [1, 2], PYTHIA [3, 4] or SHERPA [5, 6]. The Parton Branching method (PB) [7, 8], with PB-TMD distributions obtained from fits to inclusive HERA cross section measurements [9], provides an intuitive connection between parton-shower and TMD resummation.

The precise description of the transverse momentum spectrum of DY lepton pairs at low  $p_T(\ell\ell)$  at LHC energies (e.g. [10–17]) as well as at lower energies [18, 19] has been a subject for many discussions. An important role in the debate is the contribution of non-perturbative physics to the  $p_T(\ell\ell)$  spectrum at very low values, at  $p_T(\ell\ell) \lesssim 1\text{GeV}$ . In parton-shower approaches of PYTHIA and HERWIG the intrinsic- $k_T$  distribution, the transverse momentum distribution of partons at the hadron scale, plays a crucial role, and the width of this distribution is strongly dependent on the center-of-mass energy [20, 21]. On the contrary, predictions based on the PB approach give intrinsic- $k_T$  distributions which are independent (or mildly dependent) of the center-of-mass energy and the DY mass  $m_{\text{DY}}$  [22]. In Refs. [22, 23] it is argued, that this behavior comes essentially from the treatment of soft gluons, which are included in the evolution equation, and are shown to play an important role, both for the inclusive collinear parton densities as well as for the transverse momentum distributions. These soft gluons are neglected in usual parton-shower approaches by the requirement that the emitted partons should have transverse momenta of  $q_T > q_0 \simeq \mathcal{O}(\text{GeV})$ . In Refs. [24, 25] studies are being reported on a determination of the width of the intrinsic- $k_T$  distribution to be used in parton-shower event generators PYTHIA and HERWIG from measurements spanning a large range of center-of-mass energies.

In this paper we give explanations of the different behavior of the intrinsic- $k_T$  distributions in PB TMD and parton-shower approaches by including limitations on the value of  $q_T$  in calculations for TMD distributions to mimic directly what is happening in a traditional parton-shower approach. It is essential to note, that no new fits for the PB TMD have been performed, since the inclusion of a finite  $q_T$  cut would spoil the consistency of the evolution equation and the application of next-to-leading order (NLO) hard scattering cross sections, as shown in Ref. [23]. We will show explicitly that the inclusion of a finite  $q_T$  cut leads to the observed energy dependence of the width of the intrinsic- $k_T$  distribution, stressing again the importance of a proper treatment of soft gluons for inclusive distributions.

The paper is organized as follows. In Section 2 we introduce the basic concept of the PB method for TMD evolution, as well as the treatment of the small transverse momentum region within this approach. We discuss how the predictions for the transverse momentum of DY lepton pairs change with different intrinsic- $k_T$  distributions for different kinematic limits of  $q_T$ . In Section 3 we describe fits to DY data and evaluate the width of the intrinsic- $k_T$  distributions at different center-of-mass energies considering different limits of  $q_T$ . With Section 4 we conclude the paper.

## 2 PB TMDs and calculation of the DY cross section

The PB method provides an elegant way to solve the DGLAP evolution equations by an iterative method simulating explicitly each individual branching that can occur during the evolution. TMD distributions are obtained with the PB method in a direct way. Essential for this method to work is the Sudakov form factor, defined at scale  $\mu$ :

$$\Delta_a(\mu^2, \mu_0^2) = \exp \left( - \sum_b \int_{\mu_0^2}^{\mu^2} \frac{d\mathbf{q}'^2}{\mathbf{q}'^2} \int_0^{z_M} dz z P_{ba}^{(R)}(\alpha_s, z) \right), \quad (1)$$

where  $P_{ba}^{(R)}(\alpha_s, z)$  are the resolvable splitting functions for splitting of parton  $a$  into parton  $b$ , with the splitting variable  $z$  being the ratio of longitudinal momenta of the involved partons. The splitting functions are explicitly given in e.g. Ref. [7]. The parameter  $z_M$  is introduced for numerical stability with  $z_M = 1 - \epsilon$  with  $\epsilon \rightarrow 0$ . It has been shown in Ref. [7,8] that for  $\epsilon$  small enough, the DGLAP limit could be reproduced and stable solutions for the inclusive as well as TMD distributions are obtained. The importance of the large  $z$  region for inclusive and TMD distributions as well as for a parton-shower has been discussed in detail in [23].

The integral form of the PB evolution equation for a TMD density  $\mathcal{A}_a(x, \mathbf{k}, \mu^2)$  for parton  $a$  at scale  $\mu$  is given by:

$$\begin{aligned} \mathcal{A}_a(x, \mathbf{k}, \mu^2) &= \Delta_a(\mu^2) \mathcal{A}_a(x, \mathbf{k}, \mu_0^2) + \sum_b \int \frac{d^2\mathbf{q}'}{\pi\mathbf{q}'^2} \frac{\Delta_a(\mu^2)}{\Delta_a(\mathbf{q}'^2)} \Theta(\mu^2 - \mathbf{q}'^2) \Theta(\mathbf{q}'^2 - \mu_0^2) \\ &\times \int_x^{z_M} \frac{dz}{z} P_{ab}^{(R)}(\alpha_s, z) \mathcal{A}_b\left(\frac{x}{z}, \mathbf{k} + (1-z)\mathbf{q}', \mathbf{q}'^2\right), \end{aligned} \quad (2)$$

with  $x$  being the longitudinal momentum fraction and  $\mathbf{k}$  being the 2-dimensional vector of the transverse momentum with  $k_T = |\mathbf{k}|$ .

The intrinsic- $k_T$  distribution is introduced at the starting scale  $\mu_0$  of the evolution through the distribution  $\mathcal{A}_a(x, \mathbf{k}, \mu_0^2)$  in eq.(2), which is a nonperturbative boundary condition to be determined from data. The TMD density  $\mathcal{A}_a(x, \mathbf{k}, \mu_0^2)$  is parametrized in terms of a collinear parton density at the starting scale and the intrinsic- $k_T$  distribution described as a Gaussian distribution of width  $\sigma$ , which is a measure of the intensity of initial intrinsic transverse motion:

$$\mathcal{A}_{0,a}(x, \mathbf{k}, \mu_0^2) = f_{0,a}(x, \mu_0^2) \cdot \exp(-k_T^2/2\sigma^2) / (2\pi\sigma^2). \quad (3)$$

The width of the Gaussian distribution  $\sigma$  is related to the parameter  $q_s$  via  $q_s = \sqrt{2}\sigma$ .

The PB method takes into account angular ordering by relating the evolution scale  $|q'| = q'$  to the transverse momentum  $q_T$ :

$$q' = q_T / (1 - z). \quad (4)$$

The transverse momentum of the parton,  $\mathbf{k}$ , is the vectorial sum of the intrinsic transverse momentum of the initial parton and all the transverse momenta emitted in the evolution process. The PB evolution equation has been used to determine collinear and TMD distributions by fits to deep-inelastic measurements at HERA [9]. Two different sets were obtained, depending of the scale choice in  $\alpha_s$ . In PB-NLO-2018 Set1 the evolution scale  $q'$  was used as scale in  $\alpha_s$ , as in DGLAP evolution calculations like QCDNUM [26], leading to collinear distributions identical to the ones obtained as HERAPDF. In PB-NLO-2018 Set2 the transverse momentum  $q_T$  was used as the scale in  $\alpha_s$ , leading to different collinear and TMD distributions. This scale choice for  $\alpha_s$  is motivated from angular ordering, and leads to two different regions: a perturbative region, with  $q_T > q_0$ , and a non-perturbative region of  $q_T < q_0$ . In order to avoid the divergency at the Landau pole,  $\alpha_s$  is frozen for  $q_T < 1$  GeV.

The requirement of the perturbative region,  $q_T > q_0$ , leads directly to a restriction of  $z$  as given by eq.(4):

$$z_{\text{dyn}} = 1 - q_0/q'. \quad (5)$$

Since the Sudakov form factor in eq.(1) is defined over the whole  $z$  region, we can define a perturbative ( $0 < z < z_{\text{dyn}}$ ) and non-perturbative ( $z_{\text{dyn}} < z < z_M$ ) Sudakov form factor [27, 28]:

$$\begin{aligned} \Delta_a(\mu^2, \mu_0^2) &= \exp\left(-\sum_b \int_{\mu_0^2}^{\mu^2} \frac{d\mathbf{q}'^2}{\mathbf{q}'^2} \int_0^{z_{\text{dyn}}} dz z P_{ba}^{(R)}(\alpha_s, z)\right) \\ &\quad \times \exp\left(-\sum_b \int_{\mu_0^2}^{\mu^2} \frac{d\mathbf{q}'^2}{\mathbf{q}'^2} \int_{z_{\text{dyn}}}^{z_M} dz z P_{ba}^{(R)}(\alpha_s, z)\right) \\ &= \Delta_a^{(P)}(\mu^2, \mu_0^2, q_0^2) \cdot \Delta_a^{(\text{NP})}(\mu^2, \mu_0^2, q_0^2). \end{aligned} \quad (6)$$

In Ref. [22] it was shown that  $\Delta_a^{(\text{NP})}$  plays an important role in inclusive and TMD distributions and in Ref. [23] it was pointed out, that neglecting  $\Delta_a^{(\text{NP})}$  can significantly affect predictions.

In parton-shower Monte Carlo event generators a minimal transverse momentum of the emitted partons is required, either in HERWIG via the angular ordering condition and parameter  $Q_g$  [2] or in PYTHIA via  $z_{max}(Q^2)$  [4]. These cuts on  $z$  remove completely  $\Delta_a^{(NP)}$  from eq.(6).

In the following we neglect  $\Delta_a^{(NP)}$  (and real emissions with  $z > z_{dyn}$ ) in the TMD evolution to mimic the behaviour of parton-shower event generators. We do not perform new fits, but use the parameters of the starting distribution of PB-NLO-2018 Set2\* and obtain new TMD parton densities, from UPDFEVLV [29], with  $q_0$  values of 1.0 and 2.0 GeV in  $z_{dyn} = 1 - q_0/q'$ . We determine the width of the intrinsic Gauss distribution  $q_s$  for the different values of  $q_0$  applying the method of Ref. [22], and check whether with  $q_0 \sim \mathcal{O}(\text{GeV})$  we obtain an energy dependence of  $q_s$  similar to the one observed in HERWIG and PYTHIA.

## 2.1 DY cross section at NLO

The DY production cross section is obtained at NLO with MADGRAPH5\_AMC@NLO [30], as described and applied in Refs. [12, 18, 22, 31] using the integrated versions of the NLO parton densities PB-NLO-2018 Set2. The HERWIG6 subtraction terms in MCatNLO are used since they are based on the same angular ordering conditions as the PB calculations [31]. The PB TMD parton densities are included in the calculation via CASCADE3 [32]. The simulated events (labeled as MCatNLO+CAS3 in the text and figures) were passed through Rivet [33] for comparison with measurements.

The region of low transverse momentum of the DY lepton pair is expected to be sensitive to the intrinsic- $k_T$  distribution. We observe that this depends significantly on the region defined by the soft-gluon resolution scale  $z_{dyn}$  which is directly related to  $q_0$ . The sensitivity of the DY cross section on the intrinsic- $k_T$  distribution increases with increasing cut-off  $q_0$ . In Fig. 1 we show a comparison of DY transverse momentum distribution as measured by CMS at  $\sqrt{s} = 13$  TeV in the  $Z$  peak region [34] with predictions obtained with the PB method with different  $q_s$  values for two different scenarios of the soft-gluon resolution scale  $z_{dyn}$  (with  $q_0 = 1$  GeV and  $q_0 = 2$  GeV).

Using data from lower  $\sqrt{s}$ , which provide finer binning of the DY cross section at low  $p_T(\ell\ell)$ , this sensitivity rapidly increases at very small  $p_T(\ell\ell)$ , as shown in Fig. 2, where the DY cross section measurements at  $\sqrt{s} = 38.8$  GeV obtained from E605 [35] are compared to predictions obtained with different  $q_s$  for two values of  $q_0$ .

## 3 Intrinsic- $k_T$ distribution for different $q_0$ values

The width of the intrinsic- $k_T$  distribution in the PB method has been determined in Ref. [22] using MCatNLO+CAS3 with the TMD set PB-NLO-2018 Set2 where  $q_0 = 0.01$  GeV in  $z_M = 1 - q_0/q'$ . The predictions were compared with a recent measurement from CMS [34] on DY transverse momentum distribution in a wide range of the DY mass  $m_{DY}$ , obtained from p

---

\*The PB-NLO-2018 Set2 was produced with  $q_0 = 0.01$  GeV.

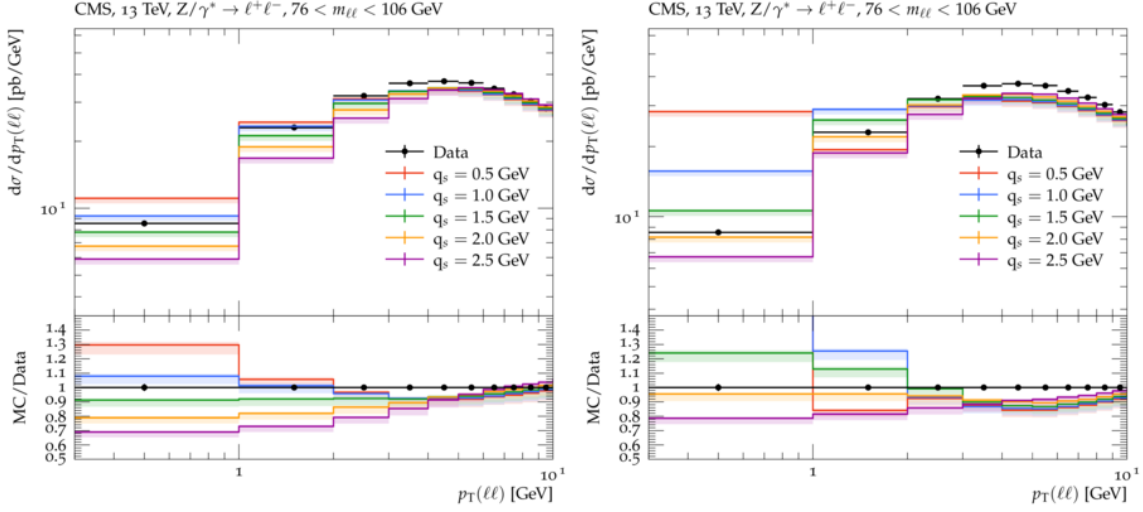


Figure 1: The DY cross section as a function of  $p_T(\ell\ell)$  in the  $Z$ -peak region as measured by CMS [34] compared to MCatNLO+CAS3 predictions with different  $q_s$ : 0.5, 1.0, 1.5, 2.0, 2.5 GeV, for the two values of  $q_0$ :  $q_0 = 1$  GeV(left) and  $q_0 = 2$  GeV(right). The bands show the scale uncertainty.

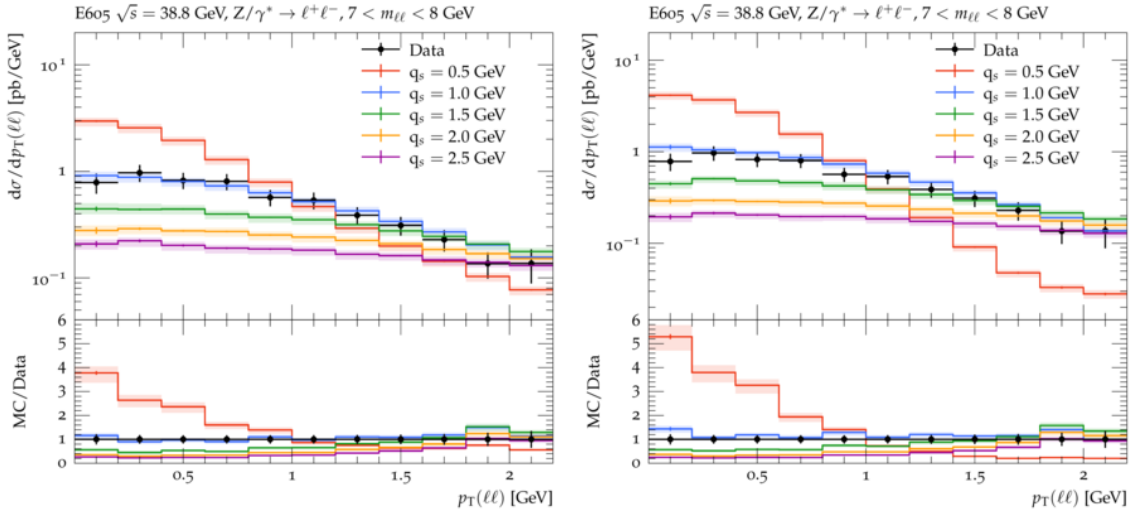


Figure 2: The DY cross section dependent on  $p_T(\ell\ell)$  as measured by E605 [35] compared to MCatNLO+CAS3 predictions with different  $q_s$ : 0.5, 1.0, 1.5, 2.0, 2.5 GeV, for the two values of  $q_0$ :  $q_0 = 1$  GeV(left) and  $q_0 = 2$  GeV(right). The bands show the scale uncertainty.

p collisions at  $\sqrt{s} = 13$  TeV. A detailed uncertainty breakdown in [22] in the five invariant mass bins allowed for a detailed fit. For comparison also DY measurements at lower  $\sqrt{s}$

were shown.

The width parameter  $q_s$  in the TMD parton distribution was varied and the predictions were compared to the measurements. To quantify the model agreement to the measurement,  $\chi^2$  is calculated:

$$\chi^2 = \sum_{i,k} (m_i - \mu_i) C_{ik}^{-1} (m_k - \mu_k) \quad (7)$$

where  $m_i$  and  $\mu_i$  are measurements and predictions from the  $i$ -th bin and  $C_{ik}$  is the covariance matrix consisting of three components: a component describing the uncertainty in the measurement, the statistical (bin by bin statistical uncertainties) and scale uncertainties in the prediction.

An optimal  $q_s$  value was obtained from the minimum of the  $\chi^2$  distribution with the best value for  $q_s$  found to be  $q_s = 1.0 \text{ GeV} \pm 0.08 \text{ GeV}$ . This result was found to be consistent with  $q_s$  values obtained from the measurements at lower center-of-mass energies and only a very mild dependence of  $q_s$  on  $\sqrt{s}$  was observed.

In the following we mimic parton-shower event generators by demanding a finite  $q_0 = 1$  and 2 GeV (without performing new fits). With such a treatment we come as close as possible to the treatment in collinear parton-shower event generators. We determine  $q_s$  from the experimental data given in Table. 1. Since most of the measurements do not provide a detailed uncertainty breakdown, we treat all the uncertainties as uncorrelated. The impact of the intrinsic- $k_T$  distribution at low collision energies has been analyzed using the entire range of  $p_T(\ell\ell)$ , while at higher center-of-mass energies, we only included bins up to the peak region ( $p_T(\ell\ell) \simeq 8 \text{ GeV}$ ) in the  $\chi^2$  calculation.

Figure 3 shows  $\chi^2 - \chi_{\min}^2$  as a function of  $q_s$  for  $q_0 = 1(2) \text{ GeV}$  for low collision energies, from about 20 to 200 GeV (27.4 GeV from E288 [36], 38.8 GeV from E605 [35] and 200 GeV from PHENIX [37]) as well as for high collision energies obtained at Tevatron and LHC (1.96 TeV from CDF [38], 8 TeV from ATLAS [39] and 13 TeV from CMS [34]). The lines shown in the figures present  $\chi^2(q_s) - \chi_{\min}^2$  with a cubic spline function interpolated through the points.

Given name	Number of bins	CM energy [GeV]	Ref.
CMS	8	13000	[34]
ATLAS	4	8000	[39]
CDF	16	1960	[38]
D0	8	1800	[40]
PHENIX	12	200	[37]
E605	11	38.8	[35]
E288	15	27.4	[36]

Table 1: List of the measurements used to determine the width of the intrinsic- $k_T$  distribution. The number of bins in  $p_T(\ell\ell)$  used in the fit as well as the collision energies are given.

From the figures one can see that with increasing collision energy the minimum of  $\chi^2(q_s) -$

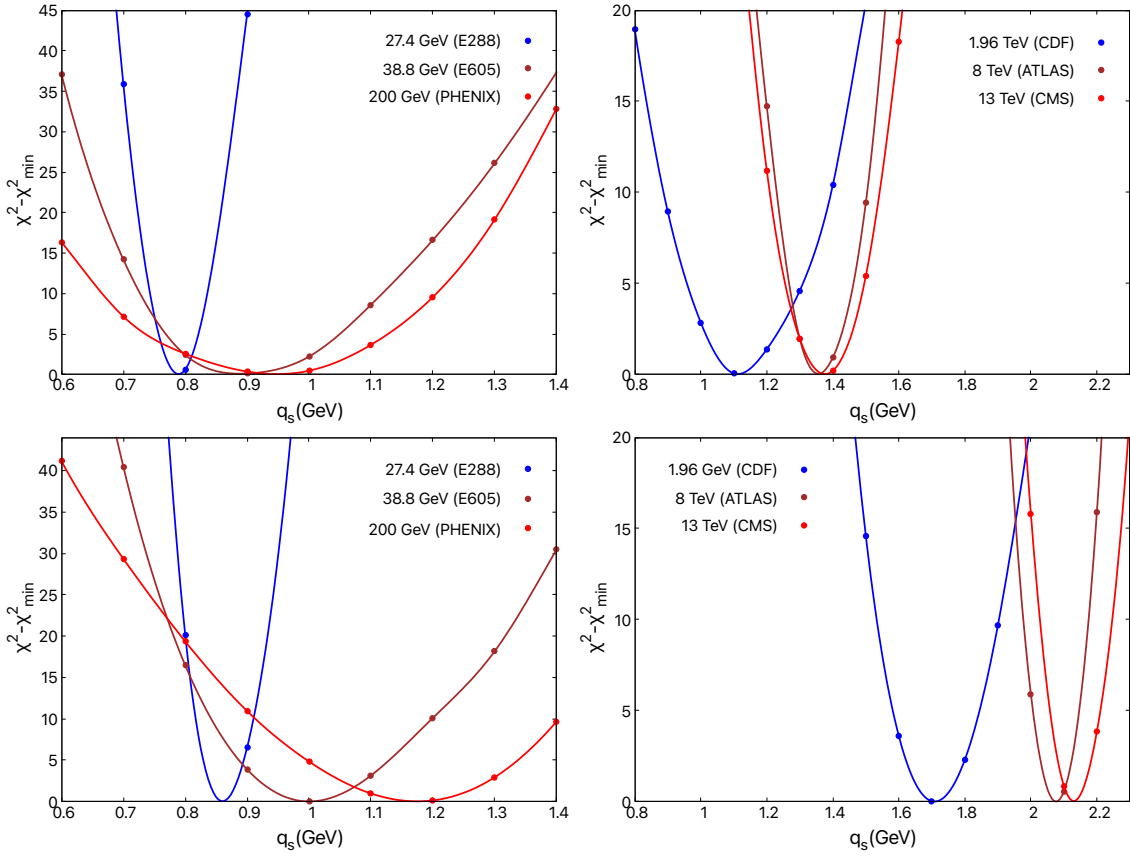


Figure 3: The  $\chi^2 - \chi_{\min}^2$  distribution as a function of  $q_s$  obtained from comparison of the MCatNLO+CAS3 prediction for  $q_0 = 1$  GeV (upper) and  $q_0 = 2$  GeV (lower) with the measurements obtained at: GeV energies [35–37] (left) and TeV energies [34,38,39] (right). Each line presents a cubic spline through the points.

$\chi_{\min}^2$  shifts to higher values of  $q_s$  ranging from 0.8 GeV to about 1.4 GeV for  $q_0 = 1$  GeV and to about 2.2 GeV for  $q_0 = 2$  GeV. The  $\chi^2/ndf$  (with  $ndf$  being the number of degrees of freedom) for all data sets is around one.

Summing up the results from  $\chi^2(q_s)$  at different center-of-mass energies, we show  $q_s$  as a function of  $\sqrt{s}$  in Fig. 4. The uncertainty for each obtained  $q_s$  value, which is determined as a position where  $\chi^2(q_s)$  has a minimum, is estimated as a range of  $q_s$  in which  $\chi^2(q_s) - \chi_{\min}^2 < 1$ . The  $q_s$  dependence on the center-of-mass energy,  $\sqrt{s}$ , for the cases with  $q_0 = 1$  GeV and  $q_0 = 2$  GeV as well as the results of Ref. [22] for the case  $q_0 = 0.01$  GeV are shown. We have performed a linear fit for the  $\log(q_s) - \log(\sqrt{s})$  relation. The uncertainty bands around the fitted lines correspond to the 95% CL band, showing the strong anti-correlation of uncertainties between intercept and slope.

We note that with higher  $q_0$  a larger fraction of soft gluons is removed with  $z < 1 - q_0/q'$



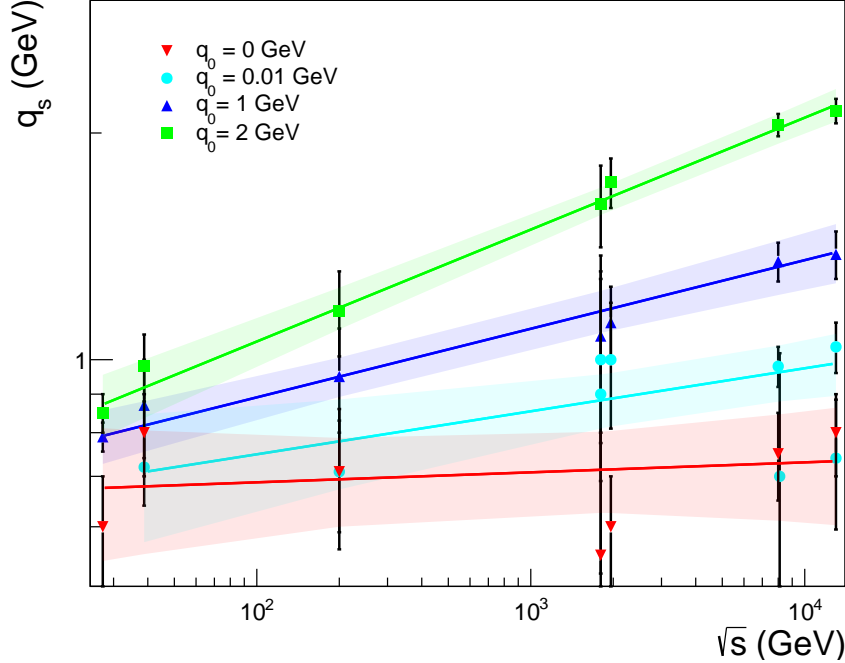


Figure 4: The  $q_s$  value as a function of collision energy,  $\sqrt{s}$ , obtained from the measurements presented in [34–40] for  $q_0 = 0.000001$  GeV,  $q_0 = 1$  GeV and  $q_0 = 2$  GeV. Also shown are results obtained from Ref. [22] for  $q_0 = 0.01$  GeV. Each line presents the linear fit of  $\log(q_s)$  vs  $\log(\sqrt{s})$ .

and therefore a larger contribution from intrinsic- $k_T$  is needed to accurately describe the transverse momentum spectrum in Drell-Yan processes. Consequently, higher  $q_0$  values lead to an increased sensitivity to the intrinsic  $k_T$ -distribution, resulting in smaller uncertainty bands.

We observe that limiting the minimal value of transverse momentum of emitted parton at each branching by  $q_0$ , a dependence of  $q_s$  on  $\sqrt{s}$  is introduced. A linear dependence of  $\log(q_s)$  on  $\log(\sqrt{s})$  is observed which is confirmed by fits with a slope increasing with increasing  $q_0$ . The result obtained in our previous study in which  $q_0 = 0.01$  GeV is consistent with a very mild  $\sqrt{s}$  dependence of  $q_s$ . In order to confirm our findings, we calculate in addition predictions for  $z_M \rightarrow 1$  with  $q_0 = 0.000001$  GeV<sup>†</sup>. The prediction with  $q_0 = 0.000001$  GeV clearly shows no  $\sqrt{s}$  dependence. We conclude, that the weak  $\sqrt{s}$  dependence observed in Ref. [22] comes from  $q_0 = 0.01$  GeV used in PB-NLO-2018 Set2 and we confirm that the dependence of the width of the intrinsic- $k_T$  distribution as a function of the center-of-mass

<sup>†</sup>We have also performed a new fit using  $q_0 = 0.000001$  GeV to the same HERA data as used in PB-NLO-2018 Set2 and found no significant differences in the collinear parton densities compared to PB-NLO-2018 Set2.

energy observed in collinear parton-shower Monte Carlo event generators comes only from the restriction of the transverse momentum of emissions in the parton-shower. No additional non-perturbative effects need to be included.

## 4 Conclusion

A detailed study was performed to show the importance of soft gluon emissions in TMDs and in parton density functions in general. In this paper we confirm that the center-of-mass energy dependence of the width of the intrinsic- $k_T$  distribution observed in collinear parton-shower Monte Carlo event generators comes from the treatment of soft gluons, and in particular from the non-perturbative Sudakov region, near the soft-gluon resolution boundary.

We have studied this effect using PB TMD distributions by imposing a cut  $q_0$  restricting the  $z$ -integration range, in order to mimic the behavior of parton-shower event generators. In order to stay consistent with the cross section calculations, no new fits were performed, but rather the PB TMD was recalculated imposing different  $q_0$  using the starting distribution of PB-NLO-2018 Set2. We have shown, that by the introduction of a finite resolution scale  $q_0$  a center-of-mass energy dependent width of the intrinsic- $k_T$  distribution is required by DY measurements over a wide range of  $\sqrt{s}$ . This dependence is reflected in a linear scaling of  $\log(q_s)$  with  $\log(\sqrt{s})$  and the slope of this dependence increases with increasing of  $q_0$ .

This study emphasises the important role of soft gluons in inclusive distributions. The inclusion of the non-perturbative region  $z \rightarrow 1$  in the evolution equation as well as in the TMD evolution is essential for the description of the low  $p_T(\ell\ell)$  region in Drell-Yan production. This non-perturbative region is included by construction in PB-NLO-2018 Set2 and this leads to a width of the intrinsic  $k_T$ -distribution independent of the collision energy  $\sqrt{s}$ .

**Acknowledgments.** We are grateful for many fruitful discussions within the CASCADE group. This article is part of a national scientific project that has received funding from Montenegrin Ministry of Education, Science and Innovation. We also acknowledge funding from the European Union’s Horizon 2020 research and innovation programme under grant agreement STRONG 2020 - No 824093. A. Lelek acknowledges funding by Research Foundation-Flanders (FWO) (application number: 1272421N). S. Taheri Monfared acknowledges the support of the German Research Foundation (DFG) under grant number 467467041.

## References

- [1] J. Bellm et al., “Herwig 7.0/Herwig++ 3.0 release note”, *Eur. Phys. J. C* **76** (2016) 196, arXiv:1512.01178.
- [2] M. Bahr et al., “Herwig++: physics and manual”, *Eur. Phys. J. C* **58** (2008) 639–707, arXiv:0803.0883.

- [3] T. Sjöstrand et al., “An introduction to PYTHIA 8.2”, *Comput. Phys. Commun.* **191** (2015) 159, arXiv:1410.3012.
- [4] C. Bierlich et al., “A comprehensive guide to the physics and usage of PYTHIA 8.3”, *SciPost Phys. Codeb.* **2022** (2022) 8, arXiv:2203.11601.
- [5] Sherpa Collaboration, “Event Generation with SHERPA 2.2”, *SciPost Phys.* **7** (2019), no. 3, 034, arXiv:1905.09127.
- [6] T. Gleisberg et al., “Event generation with SHERPA 1.1”, *JHEP* **0902** (2009) 007, arXiv:0811.4622.
- [7] F. Hautmann et al., “Collinear and TMD quark and gluon densities from Parton Branching solution of QCD evolution equations”, *JHEP* **01** (2018) 070, arXiv:1708.03279.
- [8] F. Hautmann et al., “Soft-gluon resolution scale in QCD evolution equations”, *Phys. Lett. B* **772** (2017) 446, arXiv:1704.01757.
- [9] A. Bermudez Martinez et al., “Collinear and TMD parton densities from fits to precision DIS measurements in the parton branching method”, *Phys. Rev. D* **99** (2019) 074008, arXiv:1804.11152.
- [10] A. Bacchetta et al., “Unpolarized Transverse Momentum Distributions from a global fit of Drell-Yan and Semi-Inclusive Deep-Inelastic Scattering data”, arXiv:2206.07598.
- [11] A. Bacchetta et al., “Transverse-momentum-dependent parton distributions up to N<sup>3</sup>LL from Drell-Yan data”, *JHEP* **07** (2020) 117, arXiv:1912.07550.
- [12] A. Bermudez Martinez et al., “Production of Z-bosons in the parton branching method”, *Phys. Rev. D* **100** (2019) 074027, arXiv:1906.00919.
- [13] R. Gauld et al., “Transverse momentum distributions in low-mass Drell-Yan lepton pair production at NNLO QCD”, *Phys. Lett. B* **829** (2022) 137111, arXiv:2110.15839.
- [14] W. Bizon et al., “The transverse momentum spectrum of weak gauge bosons at N<sup>3</sup> LL + NNLO”, *Eur. Phys. J. C* **79** (2019), no. 10, 868, arXiv:1905.05171.
- [15] I. Scimemi, “The vector boson transverse momentum distributions”, in *56th Rencontres de Moriond on QCD and High Energy Interactions* . 5, 2022. arXiv:2205.05997.
- [16] I. Scimemi and A. Vladimirov, “Analysis of vector boson production within TMD factorization”, *Eur. Phys. J.* **C78** (2018), no. 2, 89, arXiv:1706.01473.
- [17] M. G. Echevarria, A. Idilbi, and I. Scimemi, “Factorization Theorem For Drell-Yan At Low  $q_T$  And Transverse Momentum Distributions On-The-Light-Cone”, *JHEP* **07** (2012) 002, arXiv:1111.4996.

- [18] A. Bermudez Martinez et al., “The transverse momentum spectrum of low mass Drell–Yan production at next-to-leading order in the parton branching method”, *Eur. Phys. J. C* **80** (2020) 598, arXiv:2001.06488.
- [19] A. Bacchetta et al., “Difficulties in the description of Drell-Yan processes at moderate invariant mass and high transverse momentum”, *Phys. Rev.* **D100** (2019), no. 1, 014018, arXiv:1901.06916.
- [20] S. Gieseke, M. H. Seymour, and A. Siodmok, “A Model of non-perturbative gluon emission in an initial state parton shower”, *JHEP* **06** (2008) 001, arXiv:0712.1199.
- [21] T. Sjöstrand and P. Skands, “Multiple interactions and the structure of beam remnants”, *JHEP* **03** (2004) 053, arXiv:hep-ph/0402078.
- [22] I. Bujanja et al., “The small  $k_T$  region in Drell–Yan production at next-to-leading order with the parton branching method”, *Eur. Phys. J. C* **84** (2024) 154, arXiv:2312.08655.
- [23] M. Mendizabal, F. Guzman, H. Jung, and S. Taheri Monfared, “On the role of soft gluons in collinear parton densities”, *Eur. Phys. J. C* **84** (2024) 1299, arXiv:2309.11802.
- [24] S. Taheri Monfared, “Intrinsic  $k_T$  Distribution Independence in Drell-Yan Spectra Predictions: A Novel Insight from the Parton-Branching Method”. Talk at 42nd International Symposium on Physics in Collision (PIC 2023), October, 2023.
- [25] CMS Collaboration, “Energy-scaling behavior of intrinsic transverse momentum parameters in Drell-Yan simulation”, *CMS-GEN-22-001, CERN-EP-2024-216* (09, 2024) arXiv:2409.17770.
- [26] M. Botje, “QCDNUM: fast QCD evolution and convolution”, *Comput.Phys.Commun.* **182** (2011) 490, arXiv:1005.1481.
- [27] A. B. Martinez et al., “Soft-gluon coupling and the TMD parton branching Sudakov form factor”, arXiv:2412.21116.
- [28] A. Bermudez Martinez et al., “The Parton Branching Sudakov and its relation to CSS”, *PoS EPS-HEP2023* (2024) 270.
- [29] H. Jung, A. Lelek, K. M. Figueroa, and S. Taheri Monfared, “The Parton Branching evolution package uPDFevolv2”, arXiv:2405.20185.
- [30] J. Alwall et al., “The automated computation of tree-level and next-to-leading order differential cross sections, and their matching to parton shower simulations”, *JHEP* **1407** (2014) 079, arXiv:1405.0301.

- [31] H. Yang et al., “Back-to-back azimuthal correlations in  $Z$ +jet events at high transverse momentum in the TMD parton branching method at next-to-leading order”, *Eur. Phys. J. C* **82** (2022) 755, arXiv:2204.01528.
- [32] S. Baranov et al., “CASCADE3 A Monte Carlo event generator based on TMDs”, *Eur. Phys. J. C* **81** (2021) 425, arXiv:2101.10221.
- [33] A. Buckley et al., “Rivet user manual”, *Comput. Phys. Commun.* **184** (2013) 2803, arXiv:1003.0694.
- [34] CMS Collaboration, “Measurement of the mass dependence of the transverse momentum of lepton pairs in Drell-Yan production in proton-proton collisions at  $\sqrt{s} = 13$  TeV”, *Eur. Phys. J. C* **83** (2023) 628, arXiv:2205.04897.
- [35] G. Moreno et al., “Dimuon production in proton - copper collisions at  $\sqrt{s} = 38.8$  GeV”, *Phys. Rev. D* **43** (1991) 2815.
- [36] A. S. Ito et al., “Measurement of the Continuum of Dimuons Produced in High-Energy Proton - Nucleus Collisions”, *Phys. Rev.* **D23** (1981) 604.
- [37] PHENIX Collaboration, “Measurements of  $\mu\mu$  pairs from open heavy flavor and Drell-Yan in  $p + p$  collisions at  $\sqrt{s} = 200$  GeV”, *Phys. Rev. D* **99** (2019) 072003, arXiv:1805.02448.
- [38] CDF Collaboration, “Transverse momentum cross section of  $e^+e^-$  pairs in the  $Z$ -boson region from  $p\bar{p}$  collisions at  $\sqrt{s} = 1.96$  TeV”, *Phys. Rev. D* **86** (2012) 052010, arXiv:1207.7138.
- [39] ATLAS Collaboration, “Measurement of the transverse momentum and  $\phi_\eta^*$  distributions of Drell-Yan lepton pairs in proton-proton collisions at  $\sqrt{s} = 8$  TeV with the ATLAS detector”, *Eur. Phys. J. C* **76** (2016) 291, arXiv:1512.02192.
- [40] D0 Collaboration, “Measurement of the inclusive differential cross section for  $Z$  bosons as a function of transverse momentum in  $p\bar{p}$  collisions at  $\sqrt{s} = 1.8$  TeV”, *Phys. Rev. D* **61** (2000) 032004, arXiv:hep-ex/9907009.